Annals of Finance
https://doi.org/10.1007/s10436-024-00448-3

RESEARCH ARTICLE

Option pricing in a sentiment-biased stochastic volatility model

Alessandra Cretarola[1] · **Gianna Figà-Talamanca**[2] · **Marco Patacca**[2]

Received: 28 February 2024 / Accepted: 27 May 2024

Abstract
This paper presents a Markov-modulated stochastic volatility model that captures the dependency of market regimes on investor sentiment. The main contribution lies in developing a modified version of the classical Heston model by allowing for a sentiment-driven bias in the volatility of the asset. Specifically, a two-factor Markov-modulated stochastic volatility model is proposed, integrating a diffusion coefficient in the risky asset dynamics and a correlation parameter influenced by both the volatility process and a continuous-time Markov chain accounting for the sentiment-bias. Diverging from conventional approaches in option pricing models, this framework operates under the real-world probability measure, necessitating considerations about the existence of an equivalent martingale pricing measure. The purpose of this paper is to derive a closed formula for the pricing of European-style derivatives and to fit the model on market data through a suitable calibration procedure. A comparison with the Heston benchmark model is provided for a sample of Apple, Amazon, and Bank of America stock options.

Keywords Stochastic volatility · Regime-switching · Sentiment analysis · Option pricing

JEL Classification C22 · G12 · G13

✉ Alessandra Cretarola
alessandra.cretarola@unipg.it

Gianna Figà-Talamanca
gianna.figatalamanca@unipg.it

Marco Patacca
marco.patacca@unipg.it

[1] Department of Mathematics and Computer Science, University of Perugia, Via Luigi Vanvitelli 1, 06123 Perugia, Umbria, Italy

[2] Department of Economics, University of Perugia, via Alessandro Pascoli 20, 06123 Perugia, Umbria, Italy

Published online: 22 June 2024

1 Introduction and literature review

In the realm of finance, both the stock and derivative markets are profoundly influenced by sentiment, reflecting the collective feelings and perceptions of investors which may underlie market movements. While traditional financial models often overlook the dynamic nature of markets, regime-switching models offer a nuanced approach by recognizing distinct market states or regimes characterized by specific behaviors and relationships among assets. Human behavior shapes the market, driven by emotions such as greed, fear, optimism, and pessimism; bullish periods reflect optimism, encouraging stock buying, while bearish phases driven by fear prompt selling. Behavioral finance merges psychology with economics, highlighting sentiment's role in market dynamics. Investors use sentiment-driven strategies like momentum investing, leveraging trends shaped by sentiment. Recognizing these psychological factors helps informed decision-making in financial markets.

Despite sentiment's sway in short-term dynamics, long-term investment relies on fundamental analysis. Yet, sentiment can skew perceptions, causing undervaluation or overvaluation relative to a company's fundamentals.

In the derivative market, intricately linked to broader financial markets, sentiment is a driving force that can significantly shape pricing, trading volumes, and dynamics. Derivatives, with their leverage, mirror sentiment's shifts; bullish markets lead to increased buying, while bearish markets intensify selling pressure, affecting both derivatives and underlying assets.

With the availability of social networks, specialized forums, and online news, sentiment analysis has become a common and useful technique to gauge investor perceptions and improve the analysis of economic and financial scenarios. Several data providers, such as Bloomberg and Thomson Reuters have also started computing proprietary sentiment indexes on financial assets to be delivered together with traditional figures such as price and trading volume.

From a modeling perspective, it is widely acknowledged in financial literature that classical diffusion processes fail to adequately explain various empirical findings related to asset return time series, such as heavy tails, skewness, and volatility clustering. Potential enhancements to these models include incorporating a jump component, such as the addition of a Poisson process, as demonstrated in the seminal work of Merton (1976), or the inclusion of a self-exciting jump, as seen in the Hawkes process (Hawkes 1971, 2018). Recent examples include the works of Brignone and Sgarra (2020) and Njike Leunga and Hainaut (2024). Brignone et al. proposed a method for pricing Asian options in market models with risky asset dynamics driven by a Hawkes process with an exponential kernel. They showed that Arithmetic Asian option prices can be computed efficiently using a standard Monte Carlo method. Njike et al. expanded Heston's stochastic volatility model by adding a jump component driven by a Hawkes process with a kernel function defining the memory of the asset price process.

An alternative or complementary approach lies in regime-switching models. Motivated by the existence of regime-switching in real markets, as evidenced by Hamilton (1990), these models capture shifts between distinct market states characterized by varying risk-return profiles, instead of incorporating jumps. Understanding and mod-

eling transitions between regimes enhances market understanding, providing insights into potential triggers and implications, which aid risk management and contingent claims valuation. Specifically, regime-switching stochastic volatility models represent a powerful framework that captures the dynamic nature of financial markets by allowing for changes in both volatility and market regimes over time. Extensive literature exists regarding the application of regime-switching stochastic volatility models driven by a continuous-time Markov chain process to various financial problems. Recent examples include the works of Hainaut and Moraux (2019) and Kirkby and Nguyen (2020). Hainaut et al. proposed a hidden Markov chain with a finite number of states that modulates the parameters of a self-excited jump process. Each regime corresponds to a particular economic cycle, determining the expected return, diffusion coefficient, and long-run frequency of clustered jumps. Beyond studying the theoretical properties of this process, the authors proposed an empirical application by fitting the model to the S&P 500. Kirkby et al. devised a transform method that combines continuous-time Markov chain approximation with Fourier pricing techniques to evaluate Asian options within stochastic jump diffusion models. A comprehensive literature survey in this direction is beyond the scope of this paper. Nevertheless, we suggest the readers to see e.g. Biswas et al. (2018), Lin and He (2020), Xie and Deng (2022), He and Lin (2023) and references therein for recent developments in regime-switching stochastic volatility models.

This paper introduces a novel Markov-modulated stochastic volatility model, where regime states are driven by investor sentiment; in our opinion, sentiment-dependent market regimes echo the complex interplay between investor psychology and market dynamics. Bullish markets foster optimism and buying, potentially leading to asset bubbles, while bearish markets amplify selling pressures and risk aversion. Transitions between financial market regimes are often propelled by shifts in investors sentiment.

A previous study delving into this direction is Cretarola and Figà-Talamanca (2020), wherein the proposed model specification enables a state-dependent correlation parameter between asset returns and market attention.

The primary contribution of this paper lies in the development of a modified version of the classical Heston model under the real-world probability measure. Here, price volatility also varies according to regime changes associated with a sentiment indicator. Specifically, we consider a two-factor Markov-modulated stochastic volatility model, where the diffusion coefficient in the risky asset dynamics is the square root of the sum of two independent factor processes; the first stochastic volatility component is modeled by a square-root process and the second independent stochastic volatility component is driven by an observable continuous-time Markov chain describing investors sentiment, as well as the drift coefficient. In addition, the correlation parameter is not constant but rather depends on the two volatility factors. We stress that we do not aim to uncover latent regimes for the asset price volatility but rather to relate the regime states to changes in investor sentiment.

The findings presented in this paper can be extended to more comprehensive models, also including jumps, such as Bates (1996), Eraker et al. (2003), Eraker (2004), allowing for an explicit form of the generalized characteristic function. Therefore, we have chosen to use the Heston model as our benchmark for its simplicity and widespread use in the field.

It is worth mentioning that most regime-switching stochastic volatility models are typically set under a risk-neutral probability measure. Moreover, the dependence on the Markov chain is usually incorporated into the model in the drift coefficients of the asset price process and/or its volatility dynamics, see Elliott et al. (2007), Elliott and Lian (2013), Elliott et al. (2016), Goutte et al. (2017) among others.

An explicit dependence on the Markov chain in the diffusion coefficient of the asset price dynamics is suggested in Papanicolaou and Sircar (2014), where the model analyzed includes regime switches and jumps. We differ from Papanicolaou and Sircar (2014) since our model adopts an additive form for the diffusion coefficient in the dynamics of the risky asset, unlike their multiplicative approach. Furthermore, differently from their setting, our model specification is given under the real-world probability measure; therefore, we need to address the issue of the existence of an equivalent martingale measure in order to perform the pricing procedure, see Sect. 3.

The rest of the paper is organized as follows; Sect. 2 defines the sentiment-biased price dynamics for a financial asset, Sect. 3 collects the necessary outcomes to obtain a quasi-closed pricing formula for European-style derivatives on a sentiment-biased underlying and Sect. 4 provides a numerical application of the results. Finally, Sect. 5 collects some concluding remarks. In the Appendix, we prove the main technical result on the generalized characteristic function, which is required in the pricing procedure.

2 Modeling framework

We consider a filtered probability space $(\Omega, \mathcal{F}, \mathbf{P}; \mathbb{F})$, where $\mathbb{F} := \{\mathcal{F}_t,\ t \geq 0\}$ satisfies the usual hypotheses of completeness and right continuity, and model the dynamics of the asset price process $S = \{S_t,\ t \geq 0\}$ as follows:

$$\begin{cases} \mathrm{d}S_t = \mu_t S_t \mathrm{d}t + \sqrt{u_t + a_t} S_t \mathrm{d}W_t, \quad S_0 = s \in \mathbb{R}_+, \\ \mathrm{d}u_t = \kappa(\theta - u_t)\mathrm{d}t + \xi \sqrt{u_t}\mathrm{d}B_t, \quad u_0 = u \in \mathbb{R}_+, \end{cases} \tag{2.1}$$

where $W = \{W_t,\ t \geq 0\}$ and $B = \{B_t,\ t \geq 0\}$ are correlated $\mathbb{F}$-Brownian motions, i.e. $\langle \mathrm{d}W, \mathrm{d}B \rangle_t = \rho_t \mathrm{d}t$. Following Pacati et al. (2014), the correlation factor is conveniently set to $\rho_t = \rho(t, X_t, u_t) := \rho \sqrt{\dfrac{u_t}{u_t + a_t}}$ for each $t \geq 0$, with $\rho \in (-1, 1)$. The model parameters κ, θ, ξ are positive constants satisfying the Feller condition: $2\kappa\theta \geq \xi^2$. The drift coefficient $\{\mu_t,\ t \geq 0\}$ and the volatility factor $\{a_t,\ t \geq 0\}$ are Markov-modulated through a continuous-time Markov chain $X = \{X_t,\ t \geq 0\}$ with finite state space $\mathcal{X} = \{e_1, e_2, \ldots, e_N\}$ of unit vectors in $\mathbb{R}^N$, representing a suitable measure of market sentiment on the considered asset. We assume that X is homogeneous in time, it is independent of W and B and denote by $Q = (q_{ij})_{i,j=1,\ldots,N}$ the associated Q-matrix, where q_{ij} is an infinitesimal intensity of X. Then, it is possible to show that X admits the following semimartingale decomposition

$$X_t = X_0 + \int_0^t Q X_u \mathrm{d}u + M_t,$$

Table 1 Assigned parameters values for the Heston model and for the sentiment-biased Heston model with two (SB Heston 2R) and three (SB Heston 3R) regimes

Model	μ	κ	θ	ξ	ρ	u_0	a_1	a_2	a_3
Heston	0.05	3	0.15	0.4	−0.7	0.04	–	–	–
SB Heston 2R	0.05	3	0.15	0.4	−0.7	0.04	0.01	0.05	–
SB Heston 3R	0.05	3	0.15	0.4	−0.7	0.04	0.01	0.03	0.05

where $M = \{M_t,\ t \geq 0\}$ is a martingale with respect to the natural filtration $\mathbb{F}^X = \{\mathcal{F}_t^X,\ t \geq 0\}$ of X, defined by $\mathcal{F}_t^X = \sigma(X_s,\ s \leq t)$ for each $t \geq 0$, see Elliott et al. (1995). Thus, we can write

$$\mu_t := \mu(X_t) = \langle \boldsymbol{\mu}, X_t \rangle$$
$$a_t := a(X_t) = \langle \boldsymbol{a}, X_t \rangle,$$

for every $t \geq 0$, where $\boldsymbol{\mu} := (\mu_1, \mu_2, \ldots, \mu_N) \in \mathbb{R}^N$ and $\boldsymbol{a} := (a_1, a_2, \ldots, a_N) \in \mathbb{R}_+^N$ capture the impact of X on the drift and volatility of the price process S, respectively.

We remark that when $a_t = 0$ the price volatility only depends on the square-root process u as in the original Heston model, hence we interpret this additional factor as a bias in the asset variance related to sentiment regime changes; according to this interpretation, Eq. (2.1) is referred to as a sentiment-biased stochastic volatility model. It is worth noticing that there exists a vast literature on Markov-modulated stochastic volatility models which usually assumes some of the drift coefficients in the asset or volatility dynamics to be state dependent. Many proposals, such as Elliott et al. (2016) rely on the pioneering paper Elliott et al. (2007) where the mean-reversion parameter of the instantaneous variance is assumed to switch between regimes. Since we believe that sentiment bias is short-lived, we prefer to assume a constant mean-reversion level for the variance factor and rather add a sentiment driven distortion in the diffusion coefficient of the asset price in Eq. (2.1). In the numerical exercise we provide a comparison with Elliott et al. (2016) that confirms our conjecture.

2.1 Model characteristics: a simulation exercise

In order to highlight the contribution of the sentiment-driven bias to the dynamics of the asset price, we simulate the model in (2.1) for the case of two- and three-regimes. Since we are mainly interested in the contribution of sentiment regimes to asset volatility and option prices, we set the drift parameter μ at a constant value. The simulation exercise is based on the parameters reported in Table 1 for the original and sentiment-based (SB) Heston models.

Finally, the transition matrices P and the marginal probabilities π, corresponding to two and three sentiment regimes, are set to: $P_{2reg} = \left(\begin{smallmatrix} 0.7 & 0.3 \\ 0.4 & 0.6 \end{smallmatrix}\right)$, with $\pi_{2reg} = [0.57; 0.43]$, and $P_{3reg} = \left(\begin{smallmatrix} 0.6 & 0.3 & 0.1 \\ 0.2 & 0.5 & 0.3 \\ 0.1 & 0.3 & 0.6 \end{smallmatrix}\right)$, with $\pi_{3reg} = [0.27; 0.38; 0.35]$.

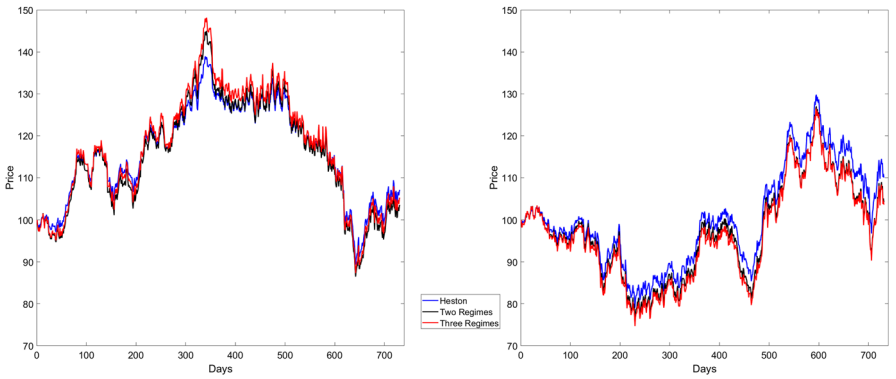

Fig. 1 Paths example for the three different model: Heston (blue line), sentiment regime switching with two-regimes (black-line) and sentiment regime switching with three-regimes (red-line) (color figure online)

In Fig. 1, we present two simulated paths illustrating asset price dynamics over a span of 2 years (730 days), assigning parameters as detailed above. These plots demonstrate how the inclusion of regimes leads to increased variability and possible shifts during specific subperiods.

For a deeper insight on model statistics, we sum up in Table 2 the basic summary statistics of daily logarithmic returns computed with respect to different time horizons T (1, 3, 6 and 12 months), on $M = 1000$ paths of the selected models. As expected, the overall contribution of sentiment bias increases with the time horizon, affecting the variability and the quantiles of the returns dynamics.

To better assess the overall contribution of the regimes to the integrated volatility, we define the annualized integrated contribution over time of sentiment bias as

$$SB(0,T) := \sqrt{\frac{1}{T}\int_0^T a(X_s)\mathrm{d}s}.$$

Fig. 2 represents the mean annualized contribution $SB(0,T)$ against different time horizons T and its empirical confidence bands at the 90% level, obtained by the simulation of $M = 1000$ different paths for the underlying Markov chain X_s, $s \leq T$.

3 Sentiment biased option pricing

In this section, we gather essential outcomes required to derive a quasi-closed pricing formula for European-style derivatives linked to a sentiment-influenced underlying. Specifically, our focus will delve into the measure transformations within the Markov-modulated Heston stochastic volatility model presented in (2.1), as well as the option pricing methodologies utilizing the conditional generalized characteristic function.

Table 2 Summary statistics of the daily logarithmic returns over different time horizons

	1 Month			3 Months			6 Months			12 Months		
	Hest	2 reg	3 reg	Hest	2 reg	3 reg	Hest	2 reg	3 reg	Hest	2 reg	3 reg
Min	−0.029	−0.040	−0.040	−0.034	−0.039	−0.039	−0.043	−0.048	−0.048	−0.038	−0.042	−0.042
Q_1	−0.006	−0.007	−0.007	−0.006	−0.007	−0.008	−0.008	−0.009	−0.009	−0.009	−0.010	−0.010
Median	0.000	0.000	0.000	−0.001	−0.001	−0.001	0.000	0.000	0.000	0.000	0.000	0.000
Mean	−0.001	−0.001	−0.001	0.000	−0.001	−0.001	0.000	0.000	0.000	0.000	0.000	0.000
Q_3	0.005	0.006	0.006	0.006	0.007	0.007	0.008	0.009	0.009	0.008	0.009	0.009
Max	0.025	0.031	0.031	0.032	0.039	0.036	0.043	0.049	0.046	0.045	0.046	0.046
Std. Dev	0.009	0.011	0.011	0.010	0.012	0.012	0.012	0.013	0.014	0.013	0.014	0.015
Skewness	−0.085	−0.105	−0.082	−0.115	−0.078	−0.086	0.075	0.082	0.072	0.127	0.115	0.112
Kurtosis	3.293	3.352	3.251	3.334	3.324	3.222	3.240	3.121	3.099	3.344	3.213	3.150
ADF p-val	0.001	0.001	0.001	0.001	0.001	0.001	0.001	0.001	0.001	0.001	0.001	0.001

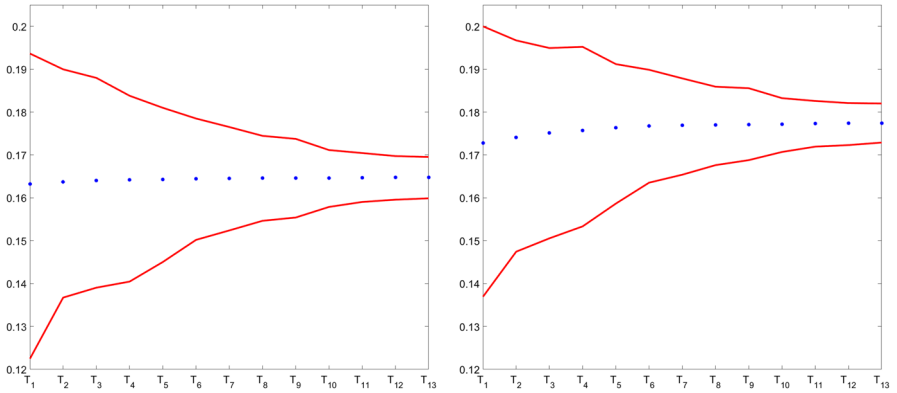

Fig. 2 Mean value of $SB(0, T)$ (blue dotted line) and 90%-confindence bands (red solid line): the two-regimes case (left plot) and the three-regimes case (right plot) (color figure online)

3.1 Risk-adjusted pricing measure

Let $T > 0$. To fix ideas, T is the expiration date of a derivative. Splitting the Brownian motion W into B and its orthogonal part $B^{\perp} = \{B_t^{\perp},\ t \geq 0\}$, we define the process $L = \{L_t,\ t \in [0, T]\}$ by

$$L_t = \exp\left\{-\int_0^t \gamma_u \mathrm{d}B_u - \int_0^t \gamma_u^{\perp} \mathrm{d}B_u^{\perp} - \frac{1}{2}\int_0^t \gamma_u^2 \mathrm{d}u - \frac{1}{2}\int_0^t (\gamma_u^{\perp})^2 \mathrm{d}u\right\},$$
$$t \in [0, T], \tag{3.1}$$

with $\gamma = \{\gamma_t,\ t \in [0, T]\}$ and $\gamma^{\perp} = \{\gamma_t^{\perp},\ t \in [0, T]\}$ satisfying proper integrability conditions. Then, the process L provides the density of a risk-neutral measure if and only if it is a true martingale and the (local) martingale property of the discounted risky asset price process holds:

$$\mu(X_t) - r = \sqrt{u_t + a(X_t)}\left(\rho_t \gamma_t + \bar{\rho}_t \gamma_t^{\perp}\right), \quad t \in [0, T], \quad \mathbf{P} - \text{a.s.}, \tag{3.2}$$

where r denotes the (constant) risk-free interest rate and we have set $\bar{\rho}_t := \sqrt{1 - \rho_t^2}$. Inspired by Heston (1993), we assume

$$\gamma_t = b\sqrt{u_t}, \quad t \in [0, T],$$

for some constant b, so that u remains in the family of square-root processes under the candidate risk-neutral measure. By substituting γ_t for $b\sqrt{u_t}$ in (3.2), we solve for $\gamma_t^{\perp}$ and since $\rho_t \in (-1, 1)$, for each $t \in [0, T]$, we get

$$\gamma_t^{\perp} = \frac{1}{\bar{\rho}_t}\left\{\frac{\mu(X_t) - r}{\sqrt{u_t + a(X_t)}} - \rho_t b\sqrt{u_t}\right\}, \quad t \in [0, T].$$

Define the constant $c := \begin{cases} 1, & \text{if } \rho = 0 \\ \min\left\{1, \dfrac{\bar{\rho}}{\rho}\right\}, & \text{if } \rho \neq 0, \end{cases}$ where $\bar{\rho} := \sqrt{1-\rho^2}$. The following result ensures that the financial market described in Sect. 2 is arbitrage-free.

Proposition 3.1 *Let L be the process given in (3.1). Then, for $|b| \leq \dfrac{\kappa}{\xi} c$ we get $\mathbb{E}[L_T] = 1$ and hence the measure $\mathbf{Q}$ defined by*

$$\left.\frac{\mathrm{d}\mathbf{Q}}{\mathrm{d}\mathbf{P}}\right|_T = L_T$$

is an equivalent martingale measure for S.

Proof To ensure that the change in measure is well defined, it is sufficient to verify that the processes γ and $\gamma^{\perp}$ satisfy the Novikov condition, i.e.

$$\mathbb{E}\left[\exp\left\{\frac{1}{2}\int_0^T \left(\gamma_s^2 + (\gamma_s^{\perp})^2\right)\mathrm{d}s\right\}\right] < \infty. \tag{3.3}$$

First, since $|b| \leq \frac{\kappa}{\xi}$, by Kraft (2005, Proposition 5.1), we get

$$\mathbb{E}\left[\exp\left\{\frac{1}{2}\int_0^T b^2 u_s \mathrm{d}s\right\}\right] < \infty,$$

which implies that the Novikov condition $\mathbb{E}\left[\exp\left\{\frac{1}{2}\int_0^T \gamma_s^2 \mathrm{d}s\right\}\right] < \infty$ is satisfied. Now, for every $t \in [0, T]$, we have

$$\begin{aligned}(\gamma_t^{\perp})^2 &= \frac{1}{(\bar{\rho}_t)^2}\left\{\frac{\mu(X_t) - r}{\sqrt{u_t + a(X_t)}} - \rho_t b\sqrt{u_t}\right\}^2 \leq \frac{2}{(\bar{\rho}_t)^2}\left\{\frac{(\mu(X_t) - r)^2}{u_t + a(X_t)} + \rho_t^2 b^2 u_t\right\} \\ &\leq \frac{2}{1-\rho^2}\left\{\frac{(\max_{j=1,\ldots,N}\langle \boldsymbol{\mu}, e_j\rangle - r)^2}{\min_{j=1,\ldots,N}\langle \boldsymbol{a}, e_j\rangle} + \rho^2 b^2 u_t\right\},\end{aligned}$$

where the last inequality holds in view of the Feller condition and because of $\rho_t^2 \leq \rho^2$, for every $t \in [0, T]$. Since $(\gamma_t^{\perp})^2$ is controlled by a quantity that is a linear function of u_t, we can write

$$(\gamma_t^{\perp})^2 \leq A + C^2 u_t, \quad t \in [0, T],$$

for some suitable constants A and C. Here, $C^2 = \dfrac{2\rho^2 b^2}{1-\rho^2}$ and it is easy to check that $C^2 \leq \frac{\kappa^2}{\xi^2}$. Then, by applying again Kraft (2005, Proposition 5.1), we get

$$\mathbb{E}\left[\exp\left\{\frac{1}{2}\int_0^T C^2 u_s \mathrm{d}s\right\}\right] < \infty,$$

which implies that $\mathbb{E}\left[\exp\left\{\frac{1}{2}\int_0^T(\gamma_s^{\perp})^2\mathrm{d}s\right\}\right] < \infty$ is satisfied and therefore, the Novikov condition (3.3) holds. □

By Girsanov's Theorem, we obtain the $\mathbf{Q}$-Brownian motions $\widetilde{B} = \left\{\widetilde{B}_t,\ t \in [0,T]\right\}$ and $\widetilde{B}^{\perp} = \left\{\widetilde{B}_t^{\perp},\ t \in [0,T]\right\}$ defined as

$$\widetilde{B}_t = B_t + \int_0^t \gamma_s \mathrm{d}s, \quad \widetilde{B}_t^{\perp} = B_t^{\perp} + \int_0^t \gamma_s^{\perp}\mathrm{d}s, \quad t \in [0,T].$$

Thanks to Proposition 3.1 we get that there are no arbitrage opportunities in the underlying financial market. Our model specification under the measure $\mathbf{Q}$ reads as

$$\begin{cases} \mathrm{d}S_t = rS_t\mathrm{d}t + \sqrt{u_t + a_t}S_t\mathrm{d}\widetilde{W}_t, & S_0 = s \in \mathbb{R}_+, \\ \mathrm{d}u_t = \alpha(\beta - u_t)\mathrm{d}t + \xi\sqrt{u_t}\mathrm{d}\widetilde{B}_t, & u_0 = u \in \mathbb{R}^+, \end{cases}$$

where $\alpha := \kappa + b\xi$, $\beta := \frac{\kappa\theta}{\kappa + b\xi}$, and $\mathrm{d}\widetilde{W}_t = \mathrm{d}W_t + (\rho_t\gamma_t + \bar{\rho}_t\gamma_t^{\perp})\mathrm{d}t$. Note that the Feller condition for the volatility process is also satisfied under $\mathbf{Q}$, since we have $2(\kappa + b\xi)\frac{\kappa\theta}{\kappa + b\xi} = 2\kappa\theta \geq \xi^2$, which is the same as under $\mathbf{P}$. Note that, since the Markov chain X is independent of W and B, its dynamics is not affected by the change of probability measure from $\mathbf{P}$ to the selected pricing measure $\mathbf{Q}$.

The above framework can be extended in order to discuss the market risk premium associated with changes in sentiment regimes. To this aim let us introduce a measure transformation for the Markov chain X and denote $H_i(t) = \mathbf{1}_{\{X_t = e_i\}}$ and $H_{ij}(t) = \sum_{0<s\leq t} H_i(s-)H_j(s)$, for $i \neq j$ with $i, j = 1, \ldots, N$; then, the process

$$M_{ij}(t) = H_{ij}(t) - q_{ij}\int_0^t H_i(s)\mathrm{d}s, \quad t \in [0,T],$$

is a $\mathbf{P}$-martingale. Moreover, consider a matrix $\tilde{\kappa} = (\tilde{\kappa}_{ij})_{i,j=1,\ldots,N}$ with elements in $\mathbb{R}$ satisfying $\tilde{\kappa}_{ij} > -1$ and $\kappa_{ii} = 0$, for all $i, j = 1, \ldots, N$. Define the probability measure $\mathbf{Q}^X$ with respect to the measure $\mathbf{Q}$ on $\mathcal{F}_t^X$ with Radon-Nikodym density $\eta = \{\eta_t,\ t \in [0,T]\}$ given by

$$\eta_t = 1 + \int_0^t \sum_{i,j=1}^N \eta_{s-}\tilde{\kappa}_{ij}\mathrm{d}M_{ij}(s), \quad t \in [0,T].$$

Then, Bielecki and Rutkowski (2004, Proposition 11.2.3) implies that X is also a Markov chain under $\mathbf{Q}^X$ with generator $Q^* = (q_{ij}^*)_{i,j=1,\ldots,N}$, where

$$q_{ij}^* = q_{ij}(1 + \tilde{\kappa}_{ij}), \quad q_{ii}^* = -\sum_{j\neq i} q_{ij}^*.$$

Since the process $L\eta$, with L given in (3.1), turns out to be a $\mathbf{P}$-martingale, it provides an admissible change of measure. Here, $\tilde{\kappa}$ corresponds to the sentiment regime-switching

risk parameter. Moreover, the discounted risky asset price process $\widetilde{S} = \{e^{-rt}S_t,\ t \in [0, T]\}$ remains a martingale even under $\mathbf{Q}^X$ since its dynamics is not influenced by this measure transformation. A similar result has been also obtained in Bo et al. (2017), where a general jump-diffusion market with regime-switching is considered and a risk-neutral probability measure is derived by a combination of the Esscher transform and change of measure on time-inhomogeneous Markov chains. This observation stems from the fact that the regime-switching risk parameter $\tilde{\kappa}$ does not affect the martingale condition, as neither L nor $\widetilde{S}$ provide any information about the Markov chain.

3.2 Option pricing via the conditional generalized characteristic function

Let $\Phi^{\mathbf{Q}}_{t,T}(z) := \mathbb{E}^{\mathbf{Q}}\left[\exp\{iz\,(Y_T - Y_t)\}|\mathcal{F}_t\right]$, for $z \in \mathcal{D}_{t,T}$, be the conditional generalized characteristic function of $Y_T - Y_t$ under the probability measure $\mathbf{Q}$, where $\mathcal{D}_{t,T} \subseteq \mathbb{C}$ denotes the domain in which it is well defined.[1] Here, $\mathbb{E}^{\mathbf{Q}}[\cdot|\mathcal{F}_t]$ represents the conditional expectation with respect to $\mathbf{Q}$. The following result shows that it is possible to efficiently compute $\Phi^{\mathbf{Q}}_{t,T}$ in our model specification.

Theorem 3.2 *Let $z \in \mathcal{D}_{t,T} \subset \mathbb{C}$. Then, the conditional generalized characteristic function $\Phi^{\mathbf{Q}}_{t,T}(z) = \mathbb{E}^{\mathbf{Q}}\left[\exp\{iz\,(Y_T - Y_t)\}|\mathcal{F}_t\right]$ is given by:*

$$\Phi^{\mathbf{Q}}_{t,T}(z) = \phi_{t,T}(z) \times \phi^{\mathbf{J}}_{t,T}(\mathbf{s}(z)), \tag{3.4}$$

where

$$\phi_{t,T}(z) = \phi_{t,T}(z; x, v, t, T) := \exp\{izx + D(z;\tau)v + C(z;\tau)\}, \tag{3.5}$$

with

$$\begin{aligned}
C(z;\tau) &:= izr\tau + \frac{\alpha\beta}{\xi^2}\left((\alpha - i\rho\xi z - d)\tau - 2\log\frac{1 - ge^{-d\tau}}{1 - g}\right),\\
D(z;\tau) &:= \frac{1}{\xi^2}(\alpha - i\rho\xi z - d)\frac{1 - e^{-d\tau}}{1 - ge^{-d\tau}},\\
d &:= \sqrt{(\alpha - i\rho\xi z)^2 + \xi^2(iz + z^2)},\\
g &:= \frac{\alpha - i\rho\xi z - d}{\alpha - i\rho\xi z + d},\\
\tau &:= T - t
\end{aligned}$$

and

$$\phi^{\mathbf{J}}_{t,T}(\mathbf{s}(z)) = \langle \exp\{[Q + \mathrm{diag}\,(\mathbf{s}(z))](T - t)\}X_t, \mathbf{1}\rangle,$$

[1] Details on the conditions for existence of the conditional generalized characteristic function, see, among others, Duffie et al. (2000), Lewis (2001), Albrecher et al. (2007)

where $\mathbf{1} := (1, 1, \ldots, 1)' \in \mathbb{R}^N$ *and* $\mathrm{diag}(\mathbf{s}(z)) = \mathbf{s}(z)\, I_{N\times N}$, *with* $I_{N\times N}$ *denoting the* $N \times N$ *identity matrix,* $\mathbf{s}(z) := (s_1(z), s_2(z), \ldots, s_{N-1}(z), 0)$ *for* $s_k(z) := -\frac{iz+z^2}{2}(a_k - a_N)$, *with* $1 \le k \le N-1$.

The proof is postponed to Appendix A.

We stress that $\phi_{t,T}$ corresponds to the generalized conditional characteristic function of the log price at time T for the classical Heston model with parameters α, β, ξ; see Duffie et al. (2000), Lewis (2000), Lewis (2001) among others.

Remark 1 Analogous results can be obtained when similar sentiment biases are introduced in the drift and diffusion coefficients of several generalizations of the Heston model, as long as the generalized characteristic function of the unbiased model is well defined. Some examples are Bates (1996), Eraker et al. (2003), Eraker (2004) among others. Moreover, since the purpose of this paper is the evaluation of European-style derivatives we focused on the derivation of the **Q**-characteristic function in (3.4). Nevertheless, it is possible to obtain an similar decomposition result under the real-world probability measure **P**.

Since the generalized characteristic function is known analytically, a straightforward application of the results referenced in Carr and Madan (1999), gives the following.

Proposition 3.3 *The pricing function at time* t *of a Call Option with strike price* K *and maturity* $T > t$ *is given by*

$$C(S, u, K, T-t) = S\Pi_1 - Ke^{-r(T-t)}\Pi_2, \tag{3.6}$$

where

$$\Pi_j = \frac{1}{2} + \frac{1}{\pi}\int_0^{+\infty} \mathrm{Re}\left[\frac{e^{-iz\log K} f_j\,(T-t, \log S, u, z)}{iz}\right] \mathrm{d}z, \quad j = 1, 2$$

with

$$f_1\,(T-t, \log S, u, z) = \frac{\Phi^{\mathbb{Q}}_{t,T}(z-i)}{\Phi^{\mathbb{Q}}_{t,T}(-i)}$$

and

$$f_2\,(T-t, \log S, u, z) = \Phi^{\mathbb{Q}}_{t,T}(z),$$

with the function $\Phi^{\mathbb{Q}}_{t,T}$ *defined in (3.4). Here,* Re[ ] *denotes the real part of a complex variable.*

Note that the pricing formula given in (3.6) aligns with the classical pricing formula established in the Heston model.

In Fig. 3 we compare the implied volatility smile obtained by computing option prices with the Heston pricing formula and considering the sentiment-biased correction in

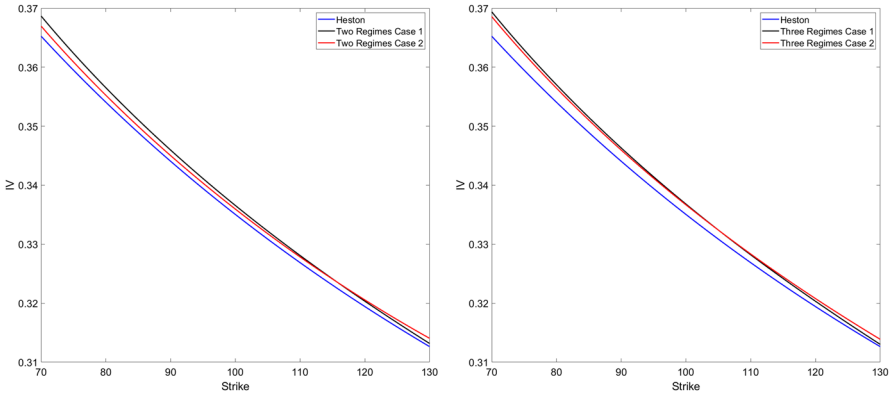

Fig. 3 Implied volatility for the Heston model and the two- and three-regimes distortions

the two- and three-regime case. In both cases the volatility dynamics parameters are assigned as in Table 1, whereas two parameter settings are considered for the regime bias: we set $a_1 = 0.01$, $a_2 = 0.05$ in two-regimes case 1, $a_1 = 0.01$, $a_2 = 0.5$ in two-regimes case 2, $a_1 = 0.03$, $a_2 = 0.01$, $a_3 = 0.05$ in three-regimes case 1 and $a_1 = 0.1$, $a_2 = 0.01$, $a_3 = 0.5$ in three-regimes case 2.

4 A numerical application on market option data

This section is dedicated to illustrating the calibration of the model specification using market data. Specifically, our focus will be on three distinct S&P 500 components. A fundamental aspect lies in identifying the sentiment regimes.

4.1 Data description

The historical sentiment based on media news for Apple (AAPL), Amazon (AMZN), and Bank of America (BAC) stocks was retrieved from Bloomberg for the period January 1, 2015, December 19, 2023. In Fig. 4 the time series for the dynamics of the sentiment score are plotted for the assets considered.

On December 19, 2023 we obtained the implied volatility smile for Apple, Amazon and Bank of America stocks from Eikon Refinitiv (now LSEG) by selecting all the options within a 30% range in moneyness and all of the available expiration dates above one week, namely $T = 16, 23, 30, 37, 58, 86, 121, 149, 184, 212, 240, 275, 366, 394, 548, 639, 730$ calendar days. We end up with a total of $M = 367, 429, 218$ options for Apple, Amazon and Bank of America, respectively. In Table 3 we report, as an example, the option data for Apple stock relative to $T = 30, 58, 86, 184, 366$ calendar days.

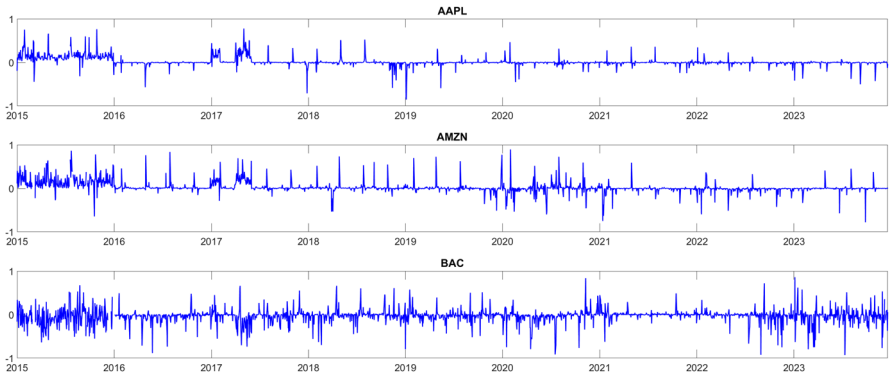

Fig. 4 News-based sentiment from January, 2015 to December 2023: Apple (top), Amazon (middle), Bank of America (bottom)

4.2 Sentiment regimes

Sentiment scores are computed by Bloomberg using proprietary algorithms and range in the continuous interval [-1,1]. For a detailed description of their computation, see Figà-Talamanca and Patacca (2022). In order to identify sentiment regimes, we discretize the value range. For the two-regimes case, positive and neutral values of the Bloomberg sentiment score are associated to the first state ("positive sentiment") of the Markov process and negative values are associated to the second state ("negative sentiment"). It is worth noticing that 10 (0.43%), 22 (0.94%) and 164 (7.01%) null values out of 2340 are observed for Apple, Amazon, and Bank of America, respectively, which need to be included either in the "positive" or in the "negative" sentiment state; we opt for the first alternative.

In the three-regimes case, we assume that the sentiment is "positive" when the score is above 0.10, is in the "neutral" state when the score belongs to the interval $]-0.10, 0.10[$, and is "negative" when below -0.10. With this interpretation, we plot in Fig. 5 the time series of the sentiment polarity for the three considered assets. Note that the selection of the threshold to assign a neutral polarity to the sentiment score (± 0.10) is arbitrary. As a robustness test, all the analyses are replicated using several threshold values. Notably, the results shows no significant changes in terms of the model pricing performance, as reported in Appendix B.

Since the regimes are derived by the Bloomberg sentiment index, the marginal probabilities are obtained by calculating the relative frequencies of being in a specific state. Similarly, each element of the transition matrix is determined by counting, for any pair $(r, s) \in \mathcal{X} \times \mathcal{X}$, the number of times for which the sentiment score moves from state r at time $t-1$ to state s at time t for any $t = 1, 2, \ldots, T$, and then dividing by the total occurrences of being in state r. In Table 4 we display the state probabilities and the transition matrices estimated for the Apple, Amazon, and Bank of America stocks in the two- and three-regimes cases, using the time series of AAPL, AMZN, and BAC sentiment indices from January 2015 to December 2019.

Table 3 Implied Volatility values (%) retrieved on December 19, 2023 for a sample of strike prices K and maturities T (in days) of Apple CALL options; the underlying price is S_0=195.89

K	$T = 30$	$T = 58$	$T = 86$	$T = 184$	$T = 366$
140	50.77	44.17	37.67	32.15	30.04
145	46.07	42.15	35.80	30.73	29.23
150	46.94	36.90	33.62	29.96	28.70
155	41.28	33.50	31.24	28.68	28.03
160	36.51	31.78	29.34	27.23	27.20
165	32.62	30.05	27.35	26.33	26.65
170	29.06	27.29	25.95	25.24	26.04
175	25.49	25.32	24.50	24.46	25.31
180	22.31	24.19	23.16	23.63	24.83
185	19.55	22.71	21.98	22.91	23.16
190	18.20	21.64	21.21	22.09	23.60
195	16.62	20.63	20.18	21.51	23.29
200	15.70	19.87	19.29	20.66	22.41
205	15.31	19.09	18.65	20.14	22.13
210	15.46	18.62	18.19	19.62	21.71
215	16.29	18.40	17.88	19.11	21.20
220	17.81	18.55	17.74	18.82	20.48
225	19.19	18.98	17.81	18.47	20.41
230	21.29	19.56	18.11	18.18	20.21
235	22.42	20.39	18.62	18.27	19.79
240	24.81	21.00	19.10	18.09	19.66
245	26.16	22.46	19.89	18.20	19.52
250	28.27	23.11	20.46	18.27	19.25

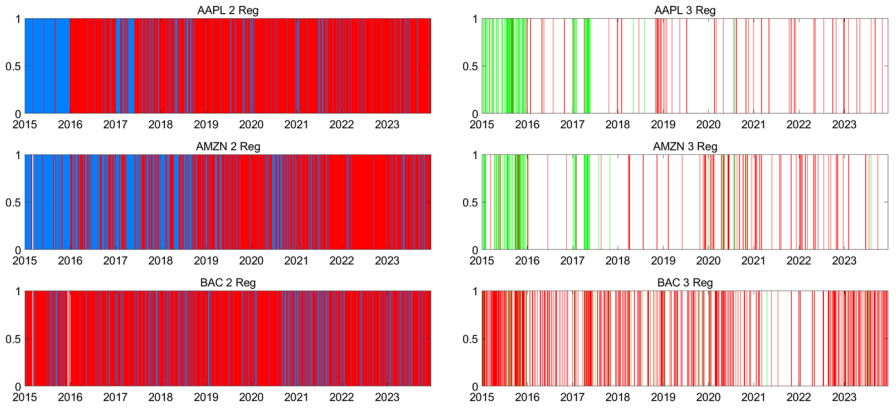

Fig. 5 Sentiment polarity from January, 2015 to December 2023 for the two-regimes (left) and three-regimes (right): Apple (top), Amazon (middle), Bank of America (bottom). Sentiment color code: Non-negative = Blue, Negative = Red, Positive = Green, Neutral = white (color figure online)

Table 4 Sentiment polarity transition matrices P and marginal probabilities π for the two- and three-regimes model applied to Apple, Amazon, and Bank of America stocks

	AAPL			AMZN			BAC		
P_{2rs}	0.644	0.356		0.734	0.266		0.498	0.502	
	0.264	0.736		0.343	0.657		0.344	0.656	
π_{2rs}	0.425	0.575		0.560	0.440		0.399	0.601	
P_{3rs}	0.710	0.258	0.032	0.600	0.371	0.029	0.274	0.493	0.234
	0.033	0.942	0.024	0.050	0.919	0.031	0.059	0.803	0.138
	0.078	0.675	0.247	0.100	0.667	0.233	0.107	0.570	0.322
π_{3rs}	0.108	0.857	0.035	0.117	0.841	0.043	0.089	0.722	0.189

4.3 Calibration

Given the quasi-closed pricing formula (3.6) in Proposition 3.3 it is possible to obtain the model parameters by minimizing a suitable loss function on a sample of M observed option prices. Since most stock options are American-style, we define the loss function based on implied volatilities rather than option prices. Precisely, given a sample $\mathbf{IV}^* = \{IV_1^*, IV_2^*, \ldots, IV_M^*, \}$ of implied volatilities derived from observed option prices, parameter values are obtained by minimizing the loss function in (4.1) below.

$$MSE(\alpha, \beta, \xi, u_0, \mathbf{a}) = \frac{1}{M} \sum_{i=1}^{M} \left(IV(\alpha, \beta, \xi, u_0, \mathbf{a}; S_0, T_i, K_i) - IV_i^* \right)^2 . \quad (4.1)$$

Calibration is performed by applying the Matlab function *lsqnonlin* to the entire data set of implied volatilities for the three considered stocks where the model implied volatility is computed assuming $S_0 = 195.89, 154.07, 33.43$ USD, for Apple, Amazon and Bank of America stocks, respectively, and $r = 5\%$. These values correspond to the asset prices and the three-month T-bill interest rate observed on December 19, 2023.

The calibrated values of the model parameters as well as the corresponding level for the Root Mean Squared Error (RMSE) are reported in Table 5.[2]

The results show consistent parameter estimates for the volatility process across the three models; the lowest RMSE is achieved by the three-regime dynamics for Amazon stocks, whereas both the two-regime and three-regime alternatives yield the same value for Apple and Bank of America. It is worth noticing that the value of the parameter a_1 is essentially 0 across all cases, suggesting that the optimal choice for the three-states model corresponds to the unbiased Heston dynamics when sentiment is positive.

[2] Note that in the calibration results, the Feller condition is violated. This occurrence is common in empirical applications when aiming for a better fit of market data, see Gatheral (2011), Guillaume and Schoutens (2010), Bakshi et al. (1997) among others. Furthermore, in our proposed model, the presence of the bias factor a_t in the diffusion coefficient makes the Feller condition less binding.

Table 5 IV Calibration results for AAPL, AMZN and BAC

	AAPL			AMZN			BAC		
	Hest	2 reg	3 reg	Hest	2 reg	3 reg	Hest	2 reg	3 reg
u_0	0.0000	0.0000	0.0000	0.0250	0.0059	0.0059	0.0856	0.0407	0.0406
β	0.0616	0.0499	0.0503	0.1176	0.1185	0.1158	0.0795	0.0959	0.0957
α	26.5780	13.9107	13.7601	21.9902	6.9075	7.0084	25.1316	5.0164	5.0875
ξ	5.0902	6.7158	6.7051	4.1695	7.0045	7.0776	6.3713	8.4271	8.4569
ρ	−0.5206	−0.6646	−0.6646	−0.3075	−0.4959	−0.5015	−0.2542	−0.3613	−0.3610
a_1	–	0.0419	0.0000	–	0.0464	0.0000	–	0.0085	0.0002
a_2	–	0.0179	0.0287	–	0.0437	0.0465	–	0.0379	0.0268
a_3	–	–	0.0178	–	–	0.1755	–	–	0.0381
RMSE	0.0170	0.0136	0.0136	0.0243	0.0201	0.0200	0.0234	0.0203	0.0203

Table 6 Historical transition rate matrix Q, calibrated forward-looking transition rate matrix Q^* and matrix $\tilde{\kappa}$ for the two-regimes model applied to Apple, Amazon, and Bank of America stocks

	AAPL		AMZN		BAC	
Q	−0.5560	0.5560	−0.4110	0.4110	−1.1074	1.1074
	0.4124	−0.4124	0.5293	−0.5293	0.7588	−0.7588
Q^*	−0.5164	0.5164	−0.4869	0.4869	−0.5089	0.5089
	0.4037	−0.4037	0.5227	−0.5227	0.3879	−0.3879
$\tilde{\kappa}$	0.0000	−0.0713	0.0000	0.1845	0.0000	−0.5404
	−0.0212	0.0000	−0.0125	0.0000	−0.4888	0.0000

We remark that the parameters reported in Table 5 are calibrated by assuming that the transition rate matrix is the one obtained under the real-world probability measure $\mathbf{P}$, i.e. by selecting the pricing measure $\mathbf{Q}$ introduced in Sect. 3.1. These results can be generalized to calibrate the transition rate matrix Q^* under the probability measure $\mathbf{Q}^X$, allowing for the computation of the risk premium associated with regime changes, defined as $\tilde{\kappa}_{ij} = \frac{q^*_{ij}}{q_{ij}} - 1$. In Table 6 we report both the transition rate matrices obtained through historical estimation (under $\mathbf{P}$) and calibration (under $\mathbf{Q}^X$), and the corresponding regime premium changes $\tilde{\kappa}$ for the three analyzed assets in the case of two regimes[3]. Note that a negative (positive) risk premium is associated to a reduction (increase) of the regime change forward-looking probability q^*_{ij} with respect to the historical value q_{ij} for $i, j = 1, 2$ with $j \neq i$. The calibration of the other parameters do not differ substantially from the values reported in Table 5.

To underscore the efficacy and utility of the sentiment-biased stochastic volatility model, we additionally calibrate the parameters and compute the calibration RMSE of the Elliott Markov-modulated variance model Elliott et al. (2016). The quoted model extends the benchmark Heston model by assuming that the mean-reversion level, representing the long-term variance to which the variance process reverts, is regime-dependent. The model we propose in this paper suggests that the "volatility bias" depending on sentiment is short-lived and affect the instantaneous rather than the long-term variance level. The calibration results and the corresponding RMSE for the Elliot model compared to our suggestion, reported in Table 7, seem to support our conjecture. Indeed, by comparing the RMSE values presented in Tables 5 and 7, it is evident that the model in (2.1) outperforms the Elliott model in all cases.[4]

To provide a deeper insight into the pricing properties on the model that we propose, Table 8 shows the values of the pricing RMSE for sub-samples of option data, categorized by maturity (5 levels) and moneyness (3 levels). Precisely we classify options as at-the-money (ATM) if their moneyness is within a 2.5% range with respect to the stock price, and as in-the-money (ITM) and out-of-the-money (OTM) if their

[3] The results for the three-regimes case are not included since this would require the estimation of six extra parameters and we believe that the available option data is nor sufficiently large to achieve calibration accuracy.

[4] We thank an anonymous reviewer for suggesting this comparison that contributes highlighting the potential of the proposed model.

Table 7 IV Calibration results for AAPL, AMZN and BAC of Elliott regime switching model

	AAPL		AMZN		BAC	
	El.2 reg	El. 3 reg	El. 2 reg	El. 3 reg	El. 2 reg	El. 3 reg
u_0	0.0754	0.1311	0.0338	0.0249	0.1783	0.1607
α	80.4891	388.1046	32.1833	67.9959	85.7067	65.8508
β_1	0.0305	0.0263	0.0930	0.0789	0.1036	0.1683
β_2	0.0555	0.0262	0.0163	0.0582	0.0215	0.0355
β_3	–	0.3587	–	0.7781	–	0.0076
ξ	4.2238	3.9959	3.3947	5.0981	5.0434	4.1260
ρ	−0.2683	0.8455	−0.1908	−0.1962	−0.0801	−0.0884
RMSE	0.0370	0.0314	0.0245	0.0225	0.0318	0.0315

moneyness is above 1.025 or below 0.975, respectively. The RMSE values are reported in the table for the Heston benchmark model and the two- and three-regime sentiment biased cases. In general, the sentiment-based specification consistently outperforms the benchmark across all groups for the analyzed stock options. with the only exceptions of Apple options for 6 months $< T \leq$ 12 months and Amazon options for 1 month $< T \leq 6$ months.

Finally, in Figs. 6, 7 and 8 we plot the observed implied volatility smile (dots) and the corresponding model curves for the Heston (blue) and the best sentiment-biased specification (red) for a sample of maturities. It is confirmed that the biased model offers a superior fit for all considered stock options.

5 Conclusions

In summary, this paper presents a Markov-modulated stochastic volatility model, driven by investor sentiment to characterize market regimes. Our specification is a modified version of the Heston model under the real-world probability measure, where price volatility dynamically responds to shifts in sentiment-influenced regimes. Precisely, the diffusion coefficient is given by the sum of a square-root-driven stochastic volatility component and a function of an observable continuous-time Markov chain representing the investor sentiment.

The main theoretical contribution of this study is the introduction of a modified version of the classical Heston model, incorporating sentiment-dependent regime changes under the real-world probability measure. This modification aims to address the dynamics of market sentiment more accurately. In discussing the existence of the risk-neutral probability measure, we ensure the absence of arbitrage opportunities within our framework. We further enhance the model's utility by deriving a quasi-closed formula for pricing European-style derivatives, leveraging the insights gained from our modified Heston model. To validate the effectiveness of our approach, we calibrate the model using data from the US market, providing empirical evidence of its applicability in real-world scenarios, and conduct a comparative analysis with the

Table 8 IV RMSE results for AAPL, AMZN and BAC

Options	AAPL				AMZN				BAC			
	Num	Hest	2 reg	3 reg	Num	Hest	2 reg	3 reg	Num	Hest	2 reg	3 reg
All	367	0.0170	0.0136	0.0136	429	0.0243	0.0201	0.0200	218	0.0234	0.0203	0.0203
$T \leq 1$	93	0.0263	0.0195	0.0195	184	0.0287	0.0208	0.0207	62	0.0353	0.0307	0.0307
$1 < T \leq 3$	67	0.0201	0.0176	0.0176	75	0.0329	0.0336	0.0336	53	0.0217	0.0192	0.0192
$3 < T \leq 6$	46	0.0095	0.0092	0.0093	56	0.0094	0.0102	0.0103	45	0.0108	0.0096	0.0096
$6 < T \leq 12$	91	0.0060	0.0071	0.0072	57	0.0102	0.0055	0.0055	50	0.0131	0.0110	0.0110
$T > 12$	70	0.0101	0.0064	0.0064	57	0.0124	0.0047	0.0046	8	0.0193	0.0143	0.0143
ITM	172	0.0214	0.0177	0.0178	203	0.0310	0.0256	0.0256	104	0.0294	0.0254	0.0254
OTM	176	0.0110	0.0082	0.0083	193	0.0156	0.0130	0.0130	88	0.0131	0.0134	0.0133
ATM	19	0.0179	0.0084	0.0084	33	0.0179	0.0144	0.0144	26	0.0232	0.0163	0.0163

The maturity ranges are expressed in months

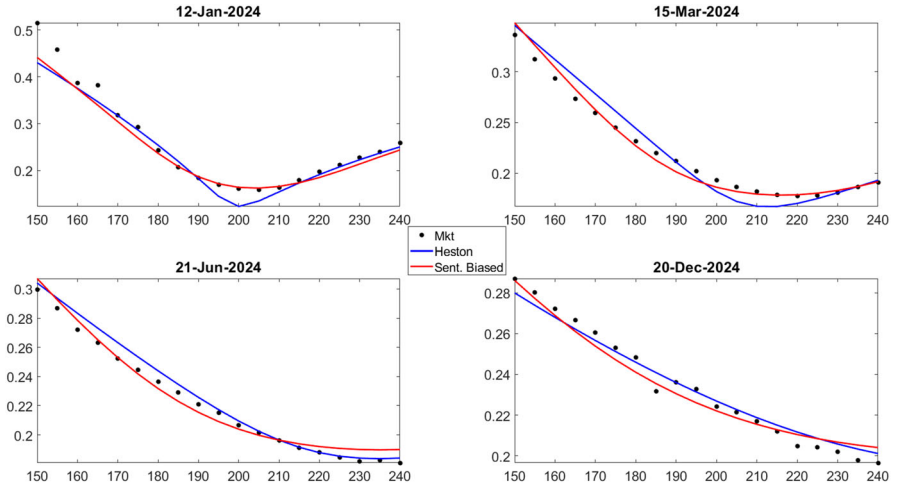

Fig. 6 AAPL model and market option smiles observed on December 19, 2023 for maturity dates T=January 12, 2024 (top-left), March 15, 2024 (top-right), June 21, 2024 (bottom-left) and December 20, 2024 (bottom-right)

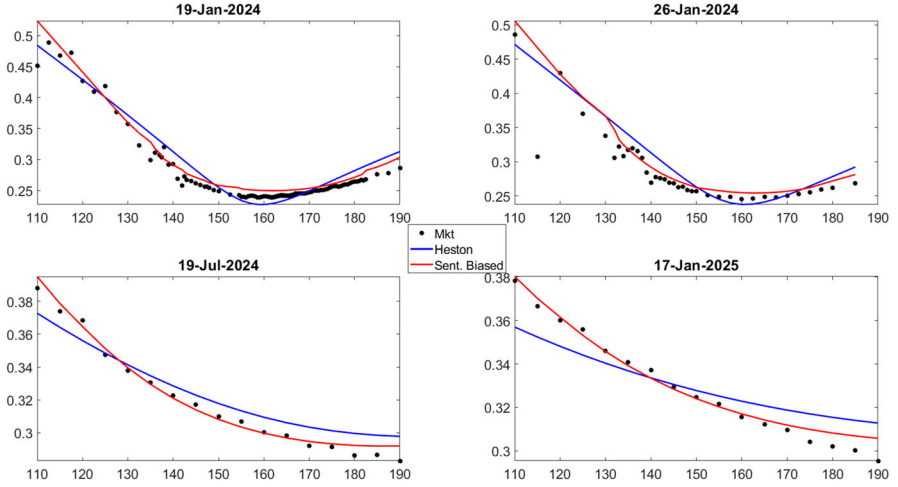

Fig. 7 AMZN model and market option smiles observed on December 19, 2023 for maturity dates T=January 19, 2024 (top-left), January 26, 2024 (top-right), July 19, 2024 (bottom-left) and January 17, 2025 (bottom-right)

Heston benchmark model to evaluate the performance of our proposed approach in capturing market dynamics and pricing derivatives effectively. A further comparison is provided with the regime-switching model in Elliott et al. (2016) which is also outperformed by our proposal.

By addressing these aspects, the study adds to the understanding of sentiment's impact on market behavior, offering insight into potential triggers, implications, and avenues for effective risk management. Indeed, regulators and risk managers recognize

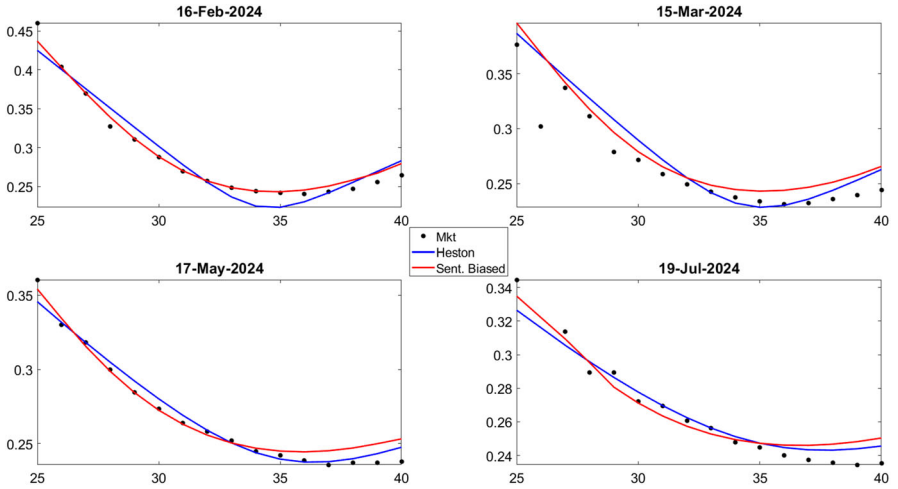

Fig. 8 BAC model and market option smiles observed on December 19, 2023 for maturity dates T=February 16, 2024 (top-left), March 15, 2024 (top-right), May 17, 2024 (bottom-left) and July 19, 2024 (bottom-right)

sentiment's significance in derivatives, monitoring for speculative risks, and systemic vulnerabilities. Integrating sentiment analysis into risk frameworks helps anticipate market scenarios and mitigate adverse impacts. The model proposed in this paper may be further extended by allowing for jumps in the asset price dynamics where either the jump intensity or the jump size can be potentially biased by investor sentiment. Finally, an interesting avenue for further investigation is the application of this approach to market indexes and to the consistent pricing of derivative products tied to the underlying stock or its volatility, measured by indices such as VIX or SPIKES (see Carr and Figà-Talamanca 2020).

A Proof of Theorem 3.2

Denote by $\mathbb{F}^{X,u} = \{\mathcal{F}_t^{X,u},\ t \geq 0\}$ the natural filtration generated by the Markov chain X and the stochastic factor u, defined by

$$\mathcal{F}_t^{X,u} := \mathcal{F}_t^X \vee \mathcal{F}_t^u, \quad t \geq 0,$$

where $\mathcal{F}_t^u = \sigma(u_s,\ s \leq t)$, for every $t \geq 0$. Let $z \in \mathcal{D}_{t,T} \subset \mathbb{C}$. The conditional generalized characteristic function $\Phi_{t,T}(z) = \mathbb{E}^{\mathbf{Q}}\left[\exp\{iz(Y_T - Y_t)\}|\mathcal{F}_t\right]$ can be easily computed by first conditioning on $\mathcal{F}_t^S \vee \mathcal{F}_T^{X,u}$, where $\mathcal{F}_t^S = \sigma(S_u,\ u \leq t)$, with $t \geq 0$. Indeed, we have

$$\Phi_{t,T}(z) = \mathbb{E}^{\mathbf{Q}}\left[\mathbb{E}^{\mathbf{Q}}\left[\exp\{iz(Y_T - Y_t)\}|\mathcal{F}_t^S \vee \mathcal{F}_T^{X,u}\right]\mathcal{F}_t\right].$$

Define the inner conditional expectation as $\Psi_{t,T}(iz) := \mathbb{E}^{\mathbf{Q}}\left[\exp\{iz\,(Y_T - Y_t)\}|\mathcal{F}_t^S \vee \mathcal{F}_T^{X,u}\right]$. Then, we have

$$\begin{aligned}\Psi_{t,T}(z) :&= \mathbb{E}^{\mathbf{Q}}\Bigg[\exp\left\{iz\int_t^T\left(r-\frac{1}{2}a(X_s)\right)\mathrm{d}s - \frac{iz}{2}\int_t^T u_s\mathrm{d}s + iz\rho\int_t^T\sqrt{u_s}\mathrm{d}B_s\right\}\\ &\quad\times\exp\left\{iz\int_t^T\sqrt{\bar{\rho}^2\,u_s + a(X_s)}\mathrm{d}B_s^{\perp}\right\}\Big|\mathcal{F}_t^S\vee\mathcal{F}_T^{X,u}\Bigg]\\ &= \exp\left\{-\frac{iz}{2}\int_t^T u_s\mathrm{d}s + iz\rho\int_t^T\sqrt{u_s}\mathrm{d}B_s + iz\int_t^T\left(r-\frac{1}{2}a(X_s)\right)\mathrm{d}s\right\}\\ &\quad\times\mathbb{E}^{\mathbf{Q}}\left[\exp\left\{iz\int_t^T\sqrt{\bar{\rho}^2\,u_s + a(X_s)}\mathrm{d}B_s^{\perp}\right\}\Big|\mathcal{F}_t^S\vee\mathcal{F}_T^{X,u}\right],\end{aligned}\tag{A.1}$$

where we recall that $\bar{\rho} = \sqrt{1-\rho^2}$. Under suitable assumptions, the latter conditional expectation is obtained as the characteristic function of a centered Gaussian distribution with variance $\int_t^T\left(\bar{\rho}^2\,u_s + a(X_s)\right)\mathrm{d}s$; hence, we have

$$\begin{aligned}&\mathbb{E}^{\mathbf{Q}}\left[\exp\left\{iz\int_t^T\sqrt{\bar{\rho}^2\,u_s + a(X_s)}\mathrm{d}B_s^{\perp}\right\}\Big|\mathcal{F}_t^S\vee\mathcal{F}_T^{X,u}\right]\\ &\quad= \exp\left\{-z^2\frac{1}{2}\int_t^T\left(\bar{\rho}^2\,u_s + a(X_s)\right)\mathrm{d}s\right\}\end{aligned}$$

and therefore (A.1) can be written as

$$\begin{aligned}\Psi_{t,T}(z) &= \exp\left\{-\frac{iz}{2}\int_t^T u_s\mathrm{d}s + iz\rho\int_t^T\sqrt{u_s}\mathrm{d}B_s + iz\int_t^T\left(r-\frac{1}{2}a(X_s)\right)\mathrm{d}s\right\}\\ &\quad\times\exp\left\{-\frac{z^2}{2}\bar{\rho}^2\int_t^T u_s\mathrm{d}s - \frac{z^2}{2}\int_t^T a(X_s)\mathrm{d}s\right\}\\ &= \exp\left\{-\frac{iz}{2}IV_{t,T} + iz\rho A_{t,T} + iz\int_t^T\left(r-\frac{1}{2}a(X_s)\right)\mathrm{d}s\right\}\\ &\quad\times\exp\left\{-\frac{z^2}{2}\bar{\rho}^2 IV_{t,T} - \frac{z^2}{2}\int_t^T a(X_s)\mathrm{d}s\right\},\end{aligned}$$

where we have set $IV_{t,T} := \int_t^T u_s\mathrm{d}s$ and

$$A_{t,T} := \int_t^T\sqrt{u_s}\mathrm{d}B_s = \frac{1}{\xi}\left(u_T - u_t - \alpha\beta(T-t) + \alpha IV_{t,T}\right).$$

Finally, in view of the independence between the processes X and u, we obtain

$$\Phi_{t,T}(z) = \mathbb{E}^{\mathbf{Q}}\Bigg[\exp\left\{-\frac{iz}{2}IV_{t,T} + iz\rho A_{t,T} + iz\int_t^T\left(r-\frac{1}{2}a(X_s)\right)\mathrm{d}s\right\}$$

$$
\begin{aligned}
&\times \exp\left\{-\frac{z^2}{2}\bar{\rho}^2 IV_{t,T} - \frac{z^2}{2}\int_t^T a(X_s)\mathrm{d}s\right\}\Big|\mathcal{F}_t\Big] \\
&= \mathbb{E}^{\mathbf{Q}}\left[\exp\left\{izr(T-t) - \frac{iz}{2}IV_{t,T} + iz\rho A_{t,T} - \frac{z^2}{2}\bar{\rho}^2 IV_{t,T}\right\}\Big|\mathcal{F}_t\right] \\
&\quad \times \mathbb{E}^{\mathbf{Q}}\left[\exp\left\{-\frac{iz}{2}\int_t^T a(X_s)\mathrm{d}s - \frac{z^2}{2}\int_t^T a(X_s)\mathrm{d}s\right\}\Big|\mathcal{F}_t\right] \\
&= \phi_{t,T}(z) \times \mathbb{E}^{\mathbf{Q}}\left[\exp\left\{-\frac{iz}{2}\int_t^T a(X_s)\mathrm{d}s - \frac{z^2}{2}\int_t^T a(X_s)\mathrm{d}s\right\}\Big|\mathcal{F}_t\right] \\
&= \phi_{t,T}(z) \times \mathbb{E}^{\mathbf{Q}}\left[\exp\left\{-\frac{iz+z^2}{2}\int_t^T a(X_s)\mathrm{d}s\right\}\Big|\mathcal{F}_t\right], \qquad \text{(A.2)}
\end{aligned}
$$

where the function $\phi_{t,T}$ is the generalized conditional characteristic function of the Heston model given in (3.5).

Now, we have to compute the latter expectation in (A.2). Note that if $\nu(X_t) = \langle \nu, X_t\rangle$ with $\nu = (\nu_1, \nu_2, \ldots, \nu_n)$, we can write

$$
\int_t^T \nu(X_s)\mathrm{d}s = \sum_{k=1}^{N} \nu_k J_k = \sum_{k=1}^{N-1} (\nu_k - \nu_N) J_k + \nu_N (T-t),
$$

where J_k is the (random) occupation time of state k within the time interval (t, T). The multivariate characteristic function of the sequence $(J_1, J_2, \ldots, J_{N-1})$ has been derived in Buffington and Elliott (2002, Lemma 1) and is given by

$$
\begin{aligned}
\phi^{\mathbf{J}}_{t,T}(\mathbf{s}) &= \mathbb{E}\left[\exp\left\{\sum_{k=1}^{N-1} s_k J_k\right\}\right] \\
&= \mathbb{E}\left[\exp\left\{\int_t^T \langle \mathbf{s}, X_u\rangle \mathrm{d}u\right\}\right] \\
&= \langle \exp\{[Q + \mathrm{diag}(\mathbf{s})](T-t)\} X_t, \mathbf{1}\rangle,
\end{aligned}
$$

where $\mathbf{s} := (s_1, s_2, \ldots, s_{N-1}, 0)$, $\mathbf{1} := (1, 1, \ldots, 1)' \in \mathbb{R}^N$ and $\mathrm{diag}(\mathbf{s}) = \mathbf{s}\, I_{N\times N}$, with $I_{N\times N}$ denoting the $N \times N$ identity matrix. Finally, we get

$$
\Phi^{\mathbf{Q}}_{t,T}(z) = \phi_{t,T}(z) \times \phi^{\mathbf{J}}_{t,T}(\mathbf{s}(z)),
$$

with $\mathbf{s}(z) := (s_1(z), s_2(z), \ldots, s_{N-1}(z), 0)$ for $s_k(z) := -\frac{iz+z^2}{2}(a_k - a_N)$.

B Robustness check

See Fig. 9 and Tables. 9, 10.

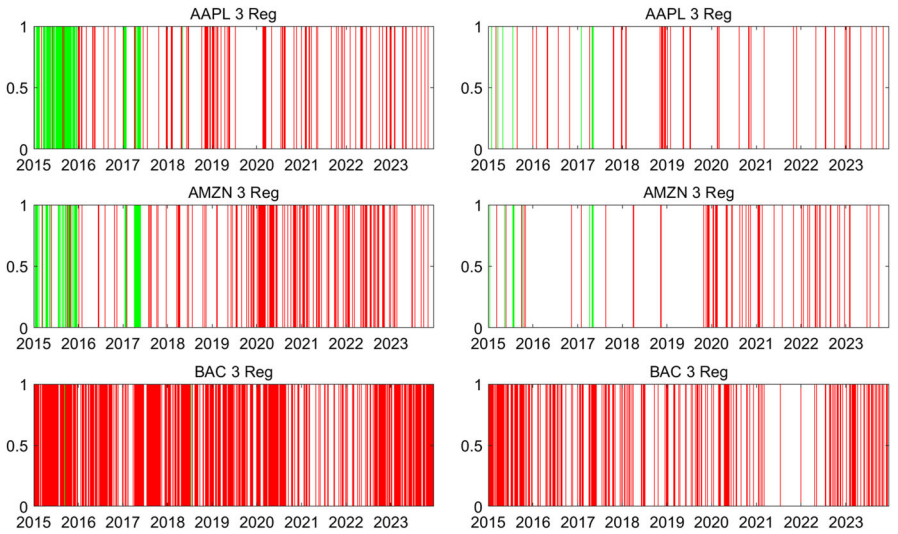

Fig. 9 Sentiment polarity from January, 2015 to December 2023 for the three-regimes with threshold 5% (left) and threshold 15% (right): Apple (top), Amazon (middle), Bank of America (bottom). Sentiment color code: Negative = Red, Positive = Green, Neutral = white

Table 9 Sentiment polarity transition matrices P and marginal probabilities π for the three-regimes model with different threshold applied to Apple, Amazon, and Bank of America stocks

	AAPL			AMZN			BAC		
Panel a: threshold 0.05									
P_{3rs}	0.849	0.119	0.032	0.672	0.287	0.041	0.306	0.407	0.287
	0.023	0.929	0.048	0.063	0.871	0.066	0.096	0.688	0.216
	0.069	0.628	0.303	0.071	0.659	0.269	0.127	0.460	0.413
π_{3rs}	0.148	0.789	0.063	0.165	0.756	0.079	0.135	0.582	0.283
Panel b: threshold 0.10									
P_{3rs}	0.710	0.258	0.032	0.600	0.371	0.029	0.274	0.493	0.234
	0.033	0.942	0.024	0.050	0.919	0.031	0.059	0.803	0.138
	0.078	0.675	0.247	0.100	0.667	0.233	0.107	0.570	0.322
π_{3rs}	0.108	0.857	0.035	0.117	0.841	0.043	0.089	0.722	0.189
Panel c: threshold 0.15									
P_{3rs}	0.524	0.453	0.024	0.423	0.551	0.026	0.239	0.606	0.155
	0.037	0.945	0.018	0.052	0.927	0.022	0.044	0.852	0.103
	0.037	0.741	0.222	0.076	0.682	0.242	0.081	0.653	0.266
π_{3rs}	0.074	0.903	0.023	0.086	0.884	0.030	0.065	0.803	0.132

Table 10 IV Calibration results for the three-regimes case of AAPL, AMZN and BAC with different threshold

	AAPL			AMZN			BAC		
	5%	10%	15%	5%	10%	15%	5%	10%	15%
u_0	0.000	0.000	0.000	0.006	0.006	0.006	0.041	0.041	0.040
β	0.050	0.050	0.046	0.113	0.116	0.117	0.095	0.096	0.099
α	13.771	13.760	15.676	7.136	7.008	6.934	5.041	5.087	4.835
ξ	6.715	6.705	6.583	7.187	7.078	7.072	8.413	8.457	8.457
ρ	−0.665	−0.665	−0.694	−0.507	−0.502	−0.500	−0.361	−0.361	−0.362
a_1	0.000	0.000	0.278	0.000	0.000	0.000	0.000	0.000	0.000
a_2	0.030	0.029	0.018	0.047	0.046	0.047	0.027	0.027	0.027
a_3	0.018	0.018	0.043	0.150	0.176	0.197	0.038	0.038	0.038
RMSE	0.014	0.014	0.014	0.020	0.020	0.020	0.020	0.020	0.020

Acknowledgements The authors are grateful to an anonymous referee for her/his objections and valuable comments that allowed to greatly improve the quality of the manuscript. The first author is member of Gruppo Nazionale per l'Analisi Matematica, la Probabilità e le loro Applicazioni (GNAMPA) of Istituto Nazionale di Alta Matematica (INdAM).

Funding The authors were partially supported by the European Union-Next Generation EU - PRIN research project n. 2022FPLY97 and by "Fondo Ricerca di Ateneo, edizione 2021".

Declarations

Conflict of interest The authors declare no potential Conflict of interest.

References

Albrecher, H., Mayer, P., Schoutens, W., Tistaert, J.: The little Heston trap. Wilmott **1**, 83–92 (2007)
Bakshi, G., Cao, C., Chen, Z.: Empirical performance of alternative option pricing models. J Financ **52**(5), 2003–2049 (1997)
Bates, D.S.: Jumps and stochastic volatility: exchange rate processes implicit in deutsche mark options. Rev Financ Stud **9**(1), 69–107 (1996)
Bielecki, T.R., Rutkowski, M.: Credit risk: modeling, valuation and hedging. Springer, Berlin (2004)
Biswas, A., Goswami, A., Overbeck, L.: Option pricing in a regime switching stochastic volatility model. Stat Probab Lett **138**, 116–126 (2018)
Bo, L., Tang, D., Wang, Y.: Optimal investment of variance-swaps in jump-diffusion market with regime-switching. J Econ Dyn Control **83**, 175–197 (2017)
Brignone, R., Sgarra, C.: Asian options pricing in Hawkes-type jump-diffusion models. Ann Financ **16**(1), 101–119 (2020)
Buffington, J., Elliott, R.J.: Regime switching and European options. In: Stochastic theory and control: proceedings of a workshop held in Lawrence, Kansas. pp. 73–82, Springer (2002)
Carr, P., Figà-Talamanca, G.: Spiking the volatility punch. Appl Math Financ **27**(6), 495–520 (2020)
Carr, P., Madan, D.: Option valuation using the fast Fourier transform. J Comput Financ **2**(4), 61–73 (1999)
Cretarola, A., Figà-Talamanca, G.: Bubble regime identification in an attention-based model for bitcoin and Ethereum price dynamics. Econ Lett **191**, 108831 (2020)
Duffie, D., Pan, J., Singleton, K.: Transform analysis and asset pricing for affine jump-diffusions. Econometrica **68**(6), 1343–1376 (2000)

Elliott, R.J., Moore, J.B., Aggoun, L.: Hidden Markov model processing. In: Hidden Markov models: estimation and control 3–11 (1995)
Elliott, R.J., Lian, G.-H.: Pricing variance and volatility swaps in a stochastic volatility model with regime switching: discrete observations case. Quant Financ **13**(5), 687–698 (2013)
Elliott, R.J., Kuen Siu, T., Chan, L.: Pricing volatility swaps under Heston's stochastic volatility model with regime switching. Appl Math Financ **14**(1), 41–62 (2007)
Elliott, R.J., Nishide, K., Osakwe, C.-J.U.: Heston-type stochastic volatility with a Markov switching regime. J Futur Mark **36**(9), 902–919 (2016)
Eraker, B.: Do stock prices and volatility jump? Reconciling evidence from spot and option prices. J Financ **59**(3), 1367–1403 (2004)
Eraker, B., Johannes, M., Polson, N.: The impact of jumps in volatility and returns. J Financ **58**(3), 1269–1300 (2003)
Figà-Talamanca, G., Patacca, M.: An explorative analysis of sentiment impact on s&p 500 components returns, volatility and downside risk. Ann Oper Res 1–23 (2022)
Gatheral, J.: The volatility surface: a practitioner's guide. Wiley, Hoboken (2011)
Goutte, S., Ismail, A., Pham, H.: Regime-switching stochastic volatility model: estimation and calibration to VIX options. Appl Math Financ **24**(1), 38–75 (2017)
Guillaume, F., Schoutens, W.: Use a reduced Heston or reduce the use of Heston? Wilmott J **2**(4), 171–192 (2010)
Hainaut, D., Moraux, F.: A switching self-exciting jump diffusion process for stock prices. Ann Financ **15**, 267–306 (2019)
Hamilton, J.D.: Analysis of time series subject to changes in regime. J Econom **45**(1–2), 39–70 (1990)
Hawkes, A.G.: Spectra of some self-exciting and mutually exciting point processes. Biometrika **58**(1), 83–90 (1971)
Hawkes, A.G.: Hawkes processes and their applications to finance: a review. Quantit Financ **18**(2), 193–198 (2018)
He, X.-J., Lin, S.: Analytically pricing exchange options with stochastic liquidity and regime switching. J Futur Mark **43**(5), 662–676 (2023)
Heston, S.L.: A closed-form solution for options with stochastic volatility with applications to bond and currency options. Rev Financ Stud **6**(2), 327–343 (1993)
Kirkby, J.L., Nguyen, D.: Efficient Asian option pricing under regime switching jump diffusions and stochastic volatility models. Ann Financ **16**(3), 307–351 (2020)
Kraft, H.: Optimal portfolios and Heston's stochastic volatility model: an explicit solution for power utility. Quant Financ **5**(3), 303–313 (2005)
Lewis, A.L.: A simple option formula for general jump-diffusion and other exponential Lévy processes. Available at SSRN 282110 (2001)
Lewis, A.L.: Option valuation under stochastic volatility. Finance Press, Newport Beach (2000)
Lin, S., He, X.-J.: Pricing variance and volatility swaps with stochastic volatility, stochastic interest rate and regime switching. Phys A **537**, 122714 (2020)
Merton, R.C.: Option pricing when underlying stock returns are discontinuous. J Financ Econ **3**(1–2), 125–144 (1976)
Njike Leunga, C.G., Hainaut, D.: Affine Heston model style with self-exciting jumps and long memory. Ann Financ **20**, 1–43 (2024)
Pacati, C., Renò, R., Santilli, M.: Heston model: shifting on the volatility surface. Risk 54–59 (2014)
Papanicolaou, A., Sircar, R.: A regime-switching Heston model for VIX and s&p 500 implied volatilities. Quant Financ **14**(10), 1811–1827 (2014)
Xie, Y., Deng, G.: Vulnerable European option pricing in a Markov regime-switching Heston model with stochastic interest rate. Chaos Solitons Fractals **156**, 111896 (2022)